AIAA 2004-2623

Active Flow Control Activities at NASA Langley

Scott G. Anders, William L. Sellers III, Anthony E. Washburn
NASA Langley Research Center
Hampton, VA

2nd AIAA Flow Control Conference
28 June - 1 July 2004
Portland, OR

Active Flow Control Activities at NASA Langley

Scott G. Anders[*], William L. Sellers III[†], and Anthony E. Washburn [‡]

NASA Langley Research Center, Hampton, VA 23681-2199

NASA Langley continues to aggressively investigate the potential advantages of active flow control over more traditional aerodynamic techniques. This paper provides an update to a previous paper and describes both the progress in the various research areas and the significant changes in the NASA research programs. The goals of the topics presented are focused on advancing the state of knowledge and understanding of controllable fundamental mechanisms in fluids as well as to address engineering challenges.

An organizational view of current research activities at NASA Langley in active flow control as supported by several projects is presented. On-center research as well as NASA Langley funded contracts and grants are discussed at a relatively high level. The products of this research are to be demonstrated either in bench-top experiments, wind-tunnel investigations, or in flight as part of the fundamental NASA R&D program and then transferred to more applied research programs within NASA, DOD, and U.S. industry.

Nomenclature

α	=	Angle of Attack (degrees)
b	=	Span (inches)
c	=	Chord
$<c_\mu>$	=	Oscillatory excitation momentum coefficient, $<J'>/cq$
C_L	=	3-D Wing lift Coefficient
C_l	=	Sectional lift Coefficient
C_d	=	Sectional drag Coefficient
C_m	=	Mass flux coefficient, kg/s, $Q\dfrac{U}{S}$
C_{mx}	=	Rolling moment coefficient
δ	=	flap deflection angle
D	=	Drag Force
f	=	Frequency, Hz
f_m	=	Modulating frequency
F^+	=	Reduced frequency, $\dfrac{(fx_{sp})}{U_\infty}$
h	=	Height of contour bump or slot height or width
J'	=	Oscillatory momentum at slot exit, $\rho h u_j'^2$
L	=	Lift force
$\dot{m}$	=	Mass flow rate, kg/s
M	=	Mach number
Q	=	Volumetric flow rate
Re	=	Reynolds number
S	=	Surface area
T	=	Thrust
U, u'	=	Mean and fluctuating velocity component
W	=	Weight
x_{sp}	=	Distance from baseline separation to reattachment

[*] Research Engineer, Flow Physics and Control Branch, M/S 170.

[†] Branch Head, Flow Physics and Control Branch, M/S 170, Associate Fellow.

[‡] Research Engineer, Flow Physics and Control Branch, M/S 170, Senior Member.

η = Thrust-vectoring efficiency, deg/percent injection
ρ = density

Abbreviations
AFC = Active Flow Control
AIP = Aerodynamic interface plane
BART = Basic Aerodynamics Research Tunnel
BLI = Boundary Layer Ingestion
BWB = Blended Wing Body
CFD = Computational Fluid Dynamics
DNS = Direct numerical simulation
DoD = Department of Defense
EET = Energy Efficient Transport
EPNdB = Effective perceived noise in dB
FLINT = Fluidic Injection Nozzle Technology
JETF = Jet Exit Test Facility
LES = Large eddy simulation
LV = Laser Velocimetry
MVGs = Micro Vortex Generators
OVERFLOW = Navier-Stokes flow solver for structured grids
PIV = Particle image Velocimetry
PJ = Zero-mass jets on port wing
PSL = Polystyrene Latex
QSP = Quiet Supersonic Platform
RANS = Reynolds averaged Navier-Stokes
SAE = Society of Automotive Engineers
SJ = Zero-mass jets on starboard wing
SOA = State-of-the-Art
SFC = Specific fuel consumption
TCT = Transonic Cryogenic Tunnel
TSFC = Thrust specific fuel consumption
URANS = Unsteady Reynolds average Navier-Stokes

Superscripts
' = Fluctuating component
max = max value

Subscripts
AM = Amplitude modulation
j = conditions at excitation slot
∞ = Freestream conditions

I. Introduction

There have been numerous studies and reviews[1,2] conducted by NASA over the last two years that look at possible visions for aeronautics and aerodynamics in the future. Included in these reviews were discussions of the future impact of increased growth in air traffic and environmental and airspace restrictions that may limit the projected growth of air travel. These impacts will result in economic loss and increased delays on airlines and increased cost and restrictions on personal air travel. In each of these reviews a bold view of the future is provided if one opens up the design space of current vehicle technology and incorporates it into a new airspace management system.

Aerodynamic research has been particularly hard hit due to the perception that it is a mature science and that only incremental gains are possible. Reference 2 discussed the aerodynamic opportunities and challenges that could provide the foundation for a revolutionary change in air vehicle technology. These included dramatic increases in computational power, artificial intelligence, active flow and noise control, computational fluid dynamics, and radical

new air vehicles that combine these technologies in a new and synergistic manner. These new technologies provide their greatest impact when included early in the design process and a need was identified for improving our conceptual design capability.

Active flow control is the main focus of this paper, and the definition of active flow control in this paper will follow the delineation proposed by Gad el Hak[3], which defines active flow control as requiring energy to be expended for control to take place. It has been stated that the greatest impact for either the airframe[2] or the engine[4], from active flow control (AFC) technology is to remove some prior barrier to a vehicle or engine concept. This paper will provide a discussion of the technologies that are being pursued at NASA Langley Research Center (LaRC) that provides some of the enabling technology for the future NASA vision. The paper updates the projects and results from Washburn[5] that summarized the prior work at Langley.

II. Goals and Organizational Structure

Any discussion of flow control at Langley should be taken in the context of the programs setting the goals and supporting the research. In this section, a description of the goals and structure of the Vehicle Systems Program (VSP) and the objectives and technology focus areas will be described.

The NASA Vehicle Systems Program has undergone major revisions in the last two years. As a result of continued pressure from Congress and the Office and Management and Budget, NASA has sought to restructure the research effort to clearly identify the return on investment through greater efficiency, accountability, and partnerships with industry and academia. The VSP has also striven to cooperate more effectively with the DoD and other government agencies, and to stress innovation through competition. The restructuring effort is being accomplished with significant input from our industrial partners and includes external review panels.

A. Aeronautics Themes for the Public Good

The key to the restructuring was to align the VSP in a simple and straightforward manner with the agency's mission, goals, themes, and objectives that are described in the NASA Strategic Plan[6]. A main thrust of the VSP is to address the agency goal to enable a safer, more secure, efficient, and environmentally friendly air transportation system. The VSP adopted four theme objectives for the public good that included, protecting the environment, increasing mobility, exploring new aerospace missions, and partnerships for national security. The environmentally friendly air transportation theme would include a major effort to protect the local and global environment by reducing aircraft noise and emissions. A brief summary of some of the environmental impacts of air transportation was provided in Ref 2. The mobility theme would include a thrust to enable more people and goods to travel faster and farther with fewer delays. The new aerospace missions theme would look to pioneer revolutionary new vehicle concepts that support science missions and terrestrial and space applications. To support and manage this research effort the VSP has put together a matrix of technology focus areas that will enable six vehicle capability sets that in turn support the aeronautics theme objectives as shown in Figure 1.

The vehicle capability sets were developed iteratively over several workshops, where various vehicle concepts and mission profiles were considered. Thirty-one vehicle concepts were originally considered at a meeting in Reno in 2003. A later meeting down selected 12 concepts and mission profiles to support the theme objectives. In discussions with various review panels that number was still considered too large and another down select reduced it to six. The vehicle capability sets that were selected for focus over the next five years included the following concepts or classes of vehicles:

- Quiet, Efficient Subsonic Transport (QuEST);

Aeronautics Theme Objectives

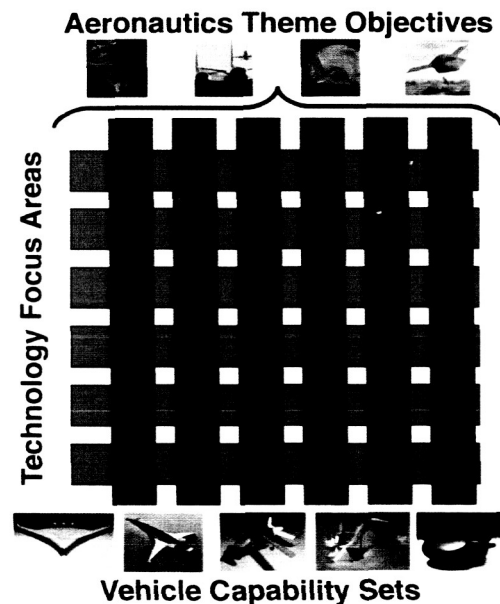**Technology Focus Areas**

Vehicle Capability Sets

Figure 1 Matrix of objectives, capability sets, and technology focus areas

- Extreme Short Takeoff & Landing Transport (ESTOL);
- Silent Small Supersonic Transport (S^4T);
- Easy-to-use, Quiet, Personal Transportation (EquiPT);
- High Altitude, Long-Endurance, Remotely Operated Aircraft (HALE ROA);
- Heavy-Lift Vertical/Short Takeoff & Landing (HeVSTOL).

In the following section the vehicle capabilities that are required to enable the QuEST, ESTOL, and S^4T missions and concepts are discussed because they will be a major focus for active flow control technology. This is not to imply that AFC will not be utilized in other areas such as EquiPT. It just means that in the prioritization process the QuEST, ESTOL, and S^4T have identified immediate areas for AFC.

B. Vehicle Capability Sets

In the down select process a set of capabilities and performance goals were identified that began with an assessment of the current state of the art and projected the required performance/vehicle improvements over a 15 year period. The Goals, Objectives, Technical Challenges, and Approaches (GOTChA) process pioneered by the DoD was used to focus research in high payoff areas to meet the overall goals of each vehicle class.

1. QuEST

The Quiet, Efficient Subsonic Transport concept has as it main goal a low-noise, low-emission, highly efficient transport aircraft. Using a Boeing 777 with GE90 engines representing the current state-of-the-art (SOA), the QuEST vehicle concept adopted the following target goals: a 50% reduction in CO_2, a 90% reduction in NOX emissions, and reducing the 65 dB noise contour to within a 55 mi^2 area representing a typical airport boundary. To meet these targets, performance goals were set to improve L/D to 25, reduce the empty weight fraction to 0.37, improve TSFC (installed @ cruise) to 0.51, and increase to 5.75 the installed engine T/W.

Several recent papers[2,7] have described the primary technologies required to reduce emissions such as CO_2, NOX, and H_2O. Reductions in CO_2 emissions are tied to reductions in fuel burn. The potential for a 50% reduction in fuel burn in the next 15 years can be

Figure 2 Potential for fuel consumption reduction over the next 20 years (from Ref. 7)

attained using a combination of aerodynamic, engine, and structural improvements as shown in Figure 2. The GOTChA process formalized which technologies are important and directly related to reaching the target goals. Active flow control can play an important role in several areas ranging from improving L/D over a wider operational range to reducing various forms of drag. Active flow control can also provide exciting new benefits when applied to an integrated airframe propulsion system. For example, ingesting the large turbulent boundary layer on a blended wing body type vehicle can provide large drag benefits. The goal is to accomplish this without presenting a highly distorted flow to the engine, which can increase high cycle fatigue and engine performance losses.
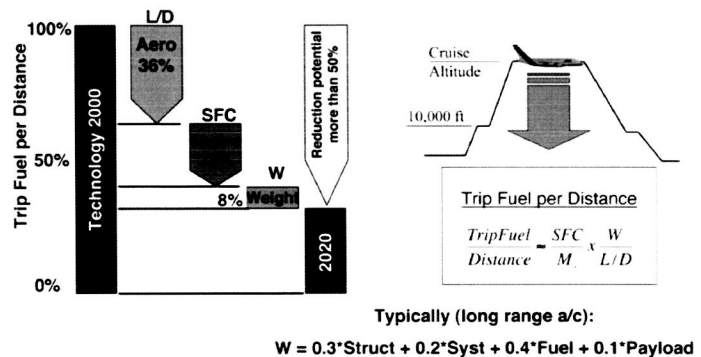
2. ESTOL

The Extreme Short Takeoff and Landing (ESTOL) concept presents a unique challenge to vehicle technology and operation. What sets this vehicle apart from previous ESTOL military-type concepts[8], are the additional requirements necessary for a successful commercial vehicle. The goal is to move from today's SOA and within the next 15 years provide the technology for a vehicle that can operate with a balanced field length of 2,000 ft, cruise at Mach 0.80, carry 90 passengers, and have a range of 1,400 nm. To accomplish this task and simultaneously open up new airports for commercial travel, the vehicle will require a takeoff and landing speed of 50 kts and a 1/4 nm turn radius in the terminal area. An ESTOL vehicle must be a good neighbor at community airports and that means that noise and efficiency will be critical considerations. By incorporating new airspace procedures with the vehicle's capabilities the goal will be to keep the objectionable noise within the airport boundary. This vehicle sector has identified specific technology targets that include a C_{Lmax} of 10, an L/D of 16, a 20 EPNdB reduction in noise from today's SOA, and reduce the empty weight fraction to 0.43. The propulsion system will need improvements in

4

engine T/W of 120% and a 10% reduction in TSFC. Improving C_{Lmax} from the current SOA of 7 will most likely require flow control and innovative new powered lift concepts. Flow control is not new to ESTOL. Wimpress[8] described the innovative leading-edge blowing and pop-up vortex generators that were coupled with the upper surface blowing on the YC-14 powered-lift system. The challenge for today is to integrate these and other technologies more efficiently using smart materials and pulsed or unsteady active flow control in an effort to avoid separation, reduce drag, and to minimize the bleed requirements from the engine.

3. S^4T

The recently retired Concorde Super Sonic Transport (SST) was a marvel of engineering for its time and provides the benchmark for the current SOA. The Mach 2.0, 3,400 nm range vehicle was restricted to supersonic travel over water due to issues regarding the sonic boom. In the future an SST will still have to deal not only with the boom issues, but also the environmental restrictions regarding emissions and takeoff and landing noise. The S^4T sector seeks to revitalize the investment in supersonic technologies and focus efforts on an efficient multi-Mach aircraft in 15-years. The concept vehicle will have a range of 5,500 nm and be able to cruise efficiently within a range of Mach numbers from 0.95 to 2.0. The 150 to 200 passenger vehicle will operate out of fields less than 8,500 ft and will generate a sonic boom signature that is acceptable for overland operations. An extremely tough set of technology goals have been set for this sector that includes an L/D of 10.5 at Mach 2.2 cruise and a takeoff L/D of 8.5. The emissions and noise requirements are equally stringent and include reducing the Stage 4 requirements by 4 EPNdB. The operating empty weight fraction has been set at 0.38 with propulsion T/W of 6. The technology areas that are receiving immediate focus include sonic boom and drag reduction. Shaping a vehicle for a tailored boom signature has been demonstrated on the highly successful DARPA Quiet Supersonic Platform (QSP) Program[9] using a modified F-5 aircraft. The S^4T sector hopes to extend that technology for the larger commercial concepts that are being considered. Drag reduction can take many forms and in the supersonic arena, laminar flow control can play a big role. NASA demonstrated[10,11] the use of hybrid laminar flow control during the F16-XL flight experiment. Using the improved understanding, new techniques, and the predictive tools available today, the hope is to develop and optimize a system that is simpler and can integrate into a low-boom configuration. Simpler and lighter high-lift systems and innovative control surfaces can provide additional weight and drag reduction benefits for this concept vehicle.

C. Strategic Technology Focus Areas

The VSP has identified six strategic technology focus areas that are matrixed into the vehicle capability sets as shown in Fig. 1 based on preliminary systems analysis and input from our industrial partners. They represent the key long-term investment areas and the primary places where technology advances will occur. A description[**] of the focus areas is provided below:

1. ***Environmentally Friendly, Clean Burning Engines:*** Developing innovative technologies to enable intelligent turbine engines that significantly reduce harmful emissions while maintaining high performance and increasing capability.
2. ***New Aircraft Energy Sources and Management:*** Developing new energy sources and intelligent management techniques directed towards zero emissions and enable new vehicle concepts for public mobility and new science missions.
3. ***Quiet Aircraft for Community Friendly Service:*** Developing and integrating noise reduction technology to enable unrestricted air transportation service to all communities.
4. ***Aerodynamic Performance for Fuel Efficiency:*** Improving aerodynamic efficiency, structures and materials technologies, and design tools and methodologies, to reduce fuel burn and minimize environmental impact and enable new vehicle concepts and capabilities for public mobility and new science missions
5. ***Aircraft Weight Reduction and Community Access:*** Developing ultra light smart materials and structures, aerodynamic concepts, and lightweight subsystems to increase vehicle efficiency, leading to high altitude long endurance vehicles, planetary aircraft, advanced vertical and short takeoff and landing vehicles and beyond.
6. ***Smart Aircraft and Autonomous Control:*** Enabling aircraft to fly with reduced or no human intervention, to optimize flight over multiple regimes, and to provide maintenance on demand towards the goal of a feeling, seeing, sensing, sentient air vehicle.

[**] Richard Wlezien: "Capability Based Research: New Horizons for Aeronautics", Invited presentation at the 42nd AIAA Aerosciences Meeting, Reno, NV, January 5th, 2004.

The technological improvements to meet the vehicle capability goals were broken into 5-year segments with clearly defined intermediate goals at the end of each 5-year segment. In the first 5-year segment, seven projects have been identified to manage and address the technology improvements for the various vehicle sector goals. These multidisciplinary projects include: Quiet Aircraft Technology (QAT), Ultra-Efficient Engine Technology (UEET), Efficient Aerodynamics Shapes and Integration (EASI), Integrated Tailored AeroStructures (ITAS), Autonomous Robust Avionics (AuRA), Low-Emission Alternative Power (LEAP), and Flight and Systems Demonstration (F&SD). The flow control activities at Langley will be discussed within the range of the projects that are supporting them.

III. Flow Control Research Topics

Flow control provides the enabling technology for many of the advanced vehicles being considered. Both passive and active technologies can play an important role. When changing flow conditions are not the critical issue, passive technologies offer the promise of simplicity. Active flow control enables optimization at off-design conditions or when it becomes necessary to react to rapidly changing flow conditions. Both active and passive flow control technologies have many potential uses on future transonic and supersonic vehicles as shown by the examples in Figure 3. Flow control provides the technology to enable improved vehicle performance, safety, and environment impact of future aircraft in both the commercial and military arena.

Figure 3   Potential uses for flow control

D. Lift Enhancement

The design of a modern high-lift system is a challenging and complex balancing act between many variables. Small changes to the high-lift system can result in large increases in performance or cost benefits. Wimpress[12] describes the balancing required for the landing, takeoff, and climb out portions of the flight vehicle and the leverage that the high-lift system provides. The landing approach speed is a function of wing loading and the maximum C_L available. To illustrate the benefits of high lift systems, Wimpress uses an example of a vehicle that is weight limited by the available field length. For takeoff, a 5% increase in C_{Lmax} results in a 20% increase in allowable payload. During climb out, L/D becomes important because sufficient thrust is required to overcome drag and climb at the required climb angle. Wimpress estimates that a 5% decrease in drag (increased L/D) results in a 40% increase in payload. In terms of landing performance, Wimpress assumes again that the vehicle is limited by landing weight. Approach speed is the most important parameter during this phase, and can be reduced by increasing C_{Lmax}. A 5% increase in C_{Lmax} results in a 65% increase in the payload carried into the field. Wimpress cautions that his estimates are simplified, but claims that the results are representative of the benefits from small improvements in high lift system performance. For a short takeoff and landing or ESTOL vehicle, aerodynamic lift is not enough to provide short field lengths; some form of powered lift is required. Wimpress shows in Figure 4 an estimate of the lift coefficients required versus field length

Figure 4   Effect of aerodynamic lift on landing distance (from Ref 12)

for a typical airplane. Circulation control or powered lift is critical to achieving field lengths less than 2,000 ft.

Simplified high lift systems can provide substantial improvements in both vehicle weight and reduced drag. System studies by Boeing[13] have shown that a high lift system consisting of a simple hinged flap with a drooped leading edge can result in a 3.3% reduction in drag and a 3.3% reduction in weight. Separation control is critical on both the leading edge and trailing edge flaps on a simplified high lift system. NASA Langley is pursuing both areas (e.g. powered lift and separation control) to support the high lift objectives of the various vehicle sectors.
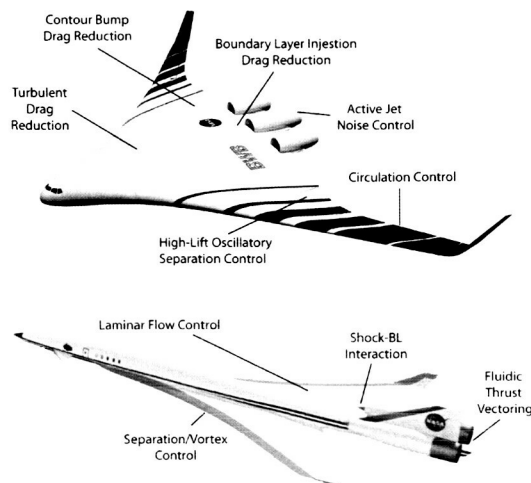
4. Separation Control

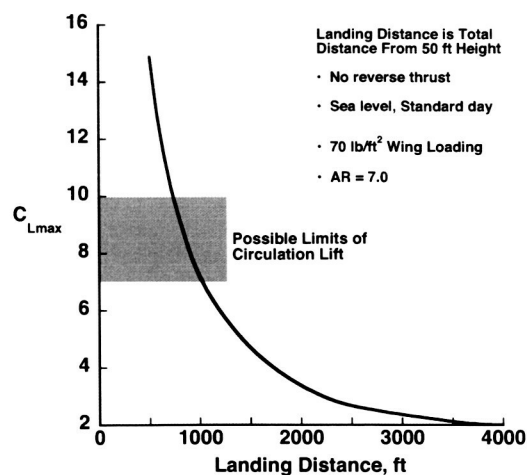Separation control is an important area of flow control research because it is so pervasive in nature, and can cause significant losses in performance. Langley has been pursuing active separation control in partnership with Tel Aviv University (TAU) for more than 5 years. The partnership builds on the pioneering experience developed at TAU on the use of oscillatory blowing for separation control. During this partnership, NASA Langley and TAU researchers took the low Reynolds number data obtained at TAU and demonstrated the technology at high Reynolds numbers on a 0015 airfoil equipped with both leading edge blowing slots and a simple trailing edge flap. As a result of that successful effort, the systems study by Boeing, described earlier, was initiated. The systems study identified the benefits, but also identified research areas that needed addressing. These areas included data using a modern supercritical wing, higher flap deflections, and the impact of any interactions when using both pulsed leading edge and flap blowing. The team conducted a series of investigations[14,15] and Washburn[16] provides a summary of their separation control research. Their research was based on the NASA Energy Efficient Transport (EET) supercritical airfoil[17] shown in Figure 5. The model was equipped with a drooped leading edge slat and a simple hinged trailing edge flap. The model was modular so that it could change blowing locations with actuators on different parts of the airfoil. The test was conducted in the NASA Langley Basic Aerodynamics Research Tunnel[18] (BART) at a freestream speed of 60 m/s (Re/m = 0.345×10^6). Figure 6 shows a picture of the model installed in the tunnel with the leading and trailing edge flaps deflected.

Pack demonstrated in Reference 14, that controlling separation on the drooped leading edge slat increased lifting capability by 12%. Amplitude modulation ($F^+_{AM} \sim 1$), of the high frequency sine wave driving the zero-net-mass actuators reduced the $<c_\mu>$ requirements by 50 percent. Controlling separation on the trailing edge flap required larger $<c_\mu>$ compared to the leading edge flap as described in Reference 15. There were important differences in performance gains when comparing combinations of pure sine and amplitude modulation of actuation on the slat and trailing edge flaps, and additional research was needed.

The most recent study[19] included a series of experiments to determine if improvements in airfoil performance could be obtained by combining multiple actuators. The effects of phase angle between actuators, duty cycle of the excitation waveform, and combining leading edge slat, trailing edge, and flap actuation (see Figure 5) were investigated. Particle image Velocimetry (PIV) data was obtained to study the large-scale structures in the flow and their interactions. The phase angles between actuation waveforms had a complex, but significant effect on both lift and drag. The results showed that the maximum lift increment occurred when the phase angle was ±30°. Figure 7 shows that combining leading edge, trailing edge and flap actuation augmented the lift over the baseline (no control) case by approximately 25% at approach angles of attack, and increased C_{lmax} by 6%. The interaction of all three actuators near C_{lmax} is very complex and requires additional study.
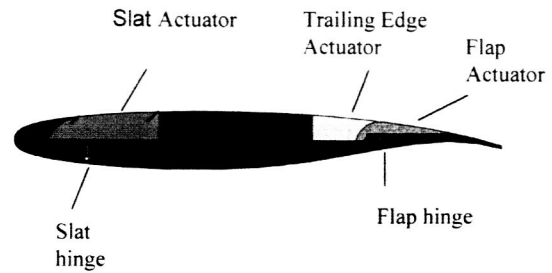

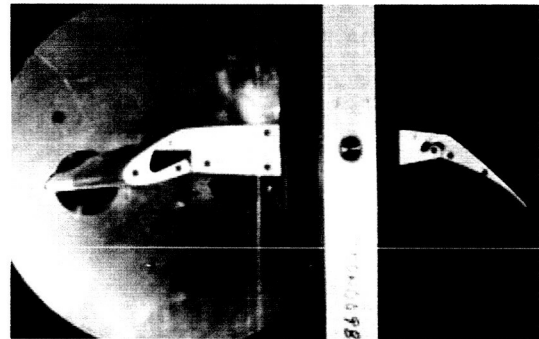**Figure 5 Modular EET model used for experiment, c=406.4mm (from Ref. 14)**

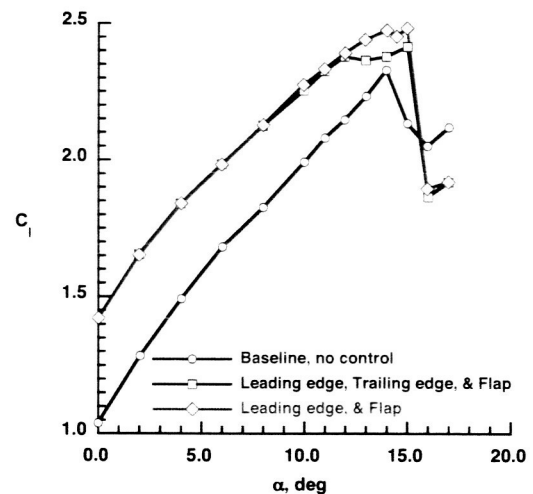**Figure 6 Simplified high lift version of EET airfoil model installed in the BART**

Figure 7 C_l versus α for various actuation locations (from Ref. 19)

5. Circulation Control

Circulation control has a proven history of success[20] in generating high lift. Because of this, circulation control is a strong candidate for integration into an ESTOL vehicle high-lift system. Past circulation control investigations have relied on steady blowing concepts to achieve significantly higher lift compared to conventional systems. However, the mass-flow requirement for steady blowing is an important concern. Therefore pulsed blowing has been investigated to see if there is potential to generate equal or greater lift with less net mass flow. Jones[21] performed pioneering research in the area of pulsed circulation control, and found that pulsed blowing reduced the mass flow requirements for ΔC_l (lift increment due to blowing) less than one. The maximum mass flow reduction[22] was 48% for a $C_l = 1.0$ ($\Delta C_l = 0.4$). Jones and Englar[23] investigated pulsed circulation control for traditional rounded Coanda surfaces (circular and elliptical) and for a dual-radius simply hinged Coanda flap. A sample of their results is shown in Figure 8. Both configurations show mass-flow reductions of about 50% for ΔC_l of 0.3 to 0.4. Their results also demonstrate that the pulsed authority, through frequency and duty cycle, can have a significant impact on the required mass flow to achieve a given performance. However, their results are limited to the boundary layer control (BLC) region shown in Figure 9. It is unknown if there is a benefit to pulsing in the super-circulation range. This is significant because the need for higher ΔC_l implies a much higher C_μ range. Unfortunately the pulsed systems did not have the authority to generate C_μ in the higher super-circulation range. Future tests at LaRC plan to address the higher pulsed C_μ range.

Jones and Englar[23] also propose solutions to the cruise drag issue for a circulation control high-lift system. The solution for the elliptical Coanda surface is to use dual-slot blowing to close the wake. For the dual-radius Coanda flap, the solution is to rotate it to zero degrees for cruise and thus close out the airfoil with a sharp trailing edge. However, all of the experimental data for these configurations are for Mach < 0.2 and Re < 500,000.

NASA Langley and the Office of Naval Research sponsored a circulation control workshop[24], in March 2004. The last circulation control workshop[25] was held in 1986 at NASA Ames. The 2004 workshop topics included applications, experiments, and computational fluid dynamics. Applications covered the terrestrial, airborne, and marine environments. The experimental results focused on aerodynamic and hydrodynamic performance and flow physics. Computation fluid dynamics focused on circulation control airfoils for marine and airborne applications. Among these was a common airfoil geometry, with experimental results, that was provided before the conference as a test case[26]. There was a very large amount of disparity in the success of matching the experimental data, even for different codes running the same turbulence models. Therefore the level of confidence in predicting circulation control performance still remains low. Efforts at NASA LaRC are concentrating on the turbulence modeling deficiencies. Plans include using a very detailed 1986 experimental dataset generated by Novak[27,28] that includes LDV measurements. The dataset was generated specifically for supporting the development of computational tools for prediction of circulation control performance.
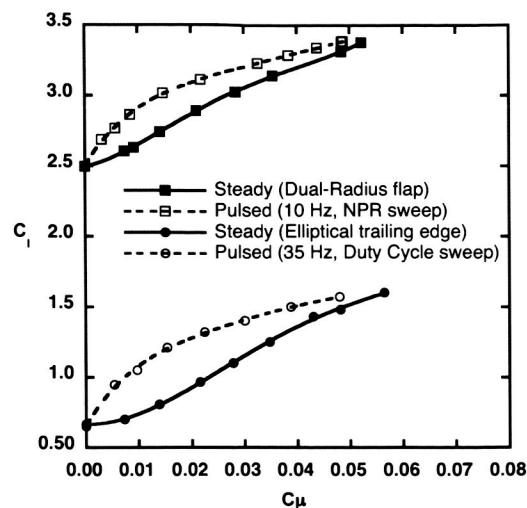

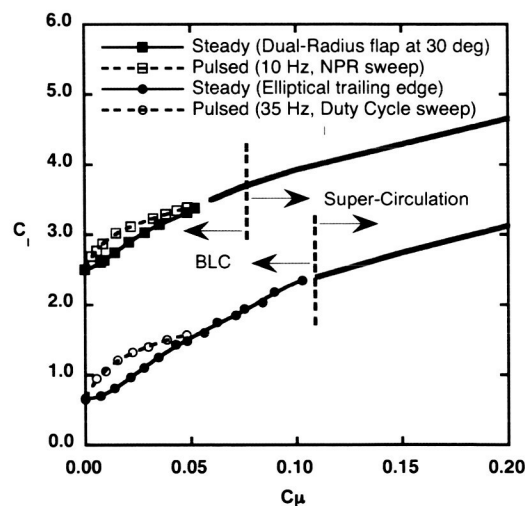**Figure 8   Comparison of pulsed and steady blowing for GTRI and LaRC CC investigations**

Figure 9   Area of super-circulation needed to obtain additional lift increment due to blowing

E. Drag Reduction

A major emphasis of the EASI project described above is the reduction of fuel burn and therefore CO_2 emissions. The drag buildup on a modern transonic aircraft is typically divided into major categories such as skin friction, induced drag, interference, and wave drag as shown in Figure 10. Skin friction and induced drag represent the bulk of the drag of a modern optimized transonic aircraft. Wave drag varies from one vehicle type to another. The EASI project is presently supporting flow control targeting skin friction and wave drag. Reduction of wave drag involves the flow physics of the interactions of shock waves and boundary layers. Skin friction reduction technology depends on whether one is working with laminar or turbulent boundary layers. Langley has a long history of laminar flow control technology that includes pioneering research and flight demonstrations of hybrid laminar flow control in both the transonic and supersonic flow regimes. In the early 80's Langley also had an extensive effort in turbulent drag reduction that

Figure 10 Breakdown of drag components (from Ref 2)

resulted in the development and flight demonstrations of passive flow control techniques such as riblets. The focus of the current turbulent drag reduction efforts is in the area of active drag reduction technologies.
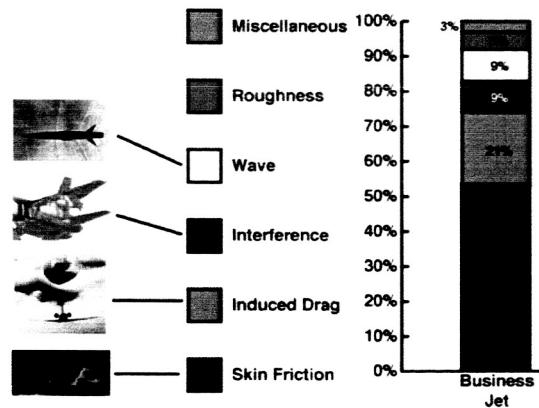
6. Shock/Boundary Layer Interaction

NASA Langley has put together a multi-disciplinary team to investigate the use of contour bumps for transonic drag reduction. The Europeans have put together an extensive investigation of the devices[29] as part of Euroshock I and II. Stanewsky[30] summarized the results and possible applications in which he discusses adaptive wing and flow control technology. The prime advantage of the contour bump technology is the reduction of wave drag at off-design conditions. These conditions become important in that a long-haul aircraft can only fly near its design point for a limited time due to the change of altitudes and weight during the flight profile. The use of localized contour bumps to actively control shock/boundary layer interactions enables the optimization of L/D over a wider range of lift coefficients and the possible increase in the buffet boundaries as described in reference 30.

The Langley effort has focused on the use of the MSES and CDISC design and optimization codes to study a family of contour bumps. To provide an accurate benchmark, a new SOA 2D transonic airfoil was designed and designated NASA TMA-0712. The airfoil has a design lift coefficient of 0.7 and a thickness to chord ratio of 12 percent. Multi-point optimization was accomplished using the MSES flow solver and the LINDOP[31] optimizer. The airfoil was also evaluated using the FUN2D viscous unstructured Navier-Stokes flow solver. The drag divergence
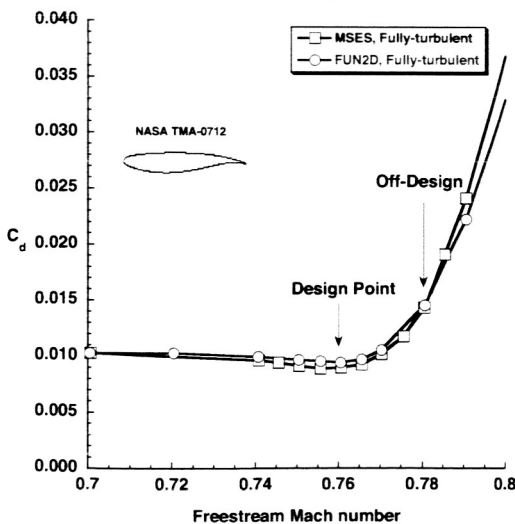
Figure 11 Drag divergence of the NASA TMA-0712 airfoil ($C_l = 0.70$, $R_e = 30 \times 10^6$)
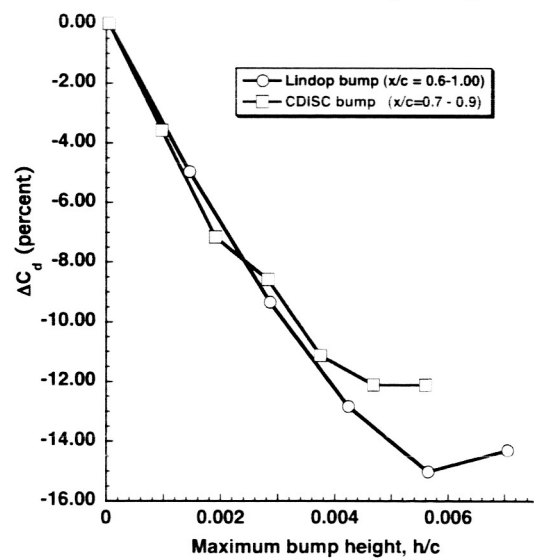
Figure 12 Drag reduction from contour bumps

9

characteristics of the airfoil are shown in Figure 11. The off-design point as defined for this study is also shown as Mach 0.78.

The contour bumps were developed using LINDOP and the CDISC[32] design code coupled with the FUN2D[33] code. The family of contour bumps was broken down into two classes based on whether they support a near-term or far-term goal. The near term goal would encompass localized bumps on the order of 20% chord that may be able to be retrofit to existing aircraft. The long-term goal would allow much larger bumps (e.g. 40% chord). The preliminary results from the investigation are very encouraging as shown in Figure 12. The results show that reductions in drag ranging from 12% to 15% depending on bump height and the length of the bump. The project is presently conducting high Reynolds number testing of the contour bumps in the NASA Langley 0.3-m Transonic Cryo Tunnel (TCT). Milholen will present a complete description of the computational and experimental results in an upcoming paper[34].

7. Active Drag Reduction

As noted earlier NASA Langley had an extensive turbulent boundary layer drag reduction program in the 1980's. That program led to the only turbulent drag reduction concept to be verified at flight conditions. The concept known as riblets showed a 6 % drag reduction in low speed tunnel tests as well as at flight conditions. Despite extensive geometric parameter studies, the maximum riblet performance was approximately 6%, which translates into approximately a 1-2 % total drag reduction if riblets were applied to a large commercial transport. Although a 1-2% reduction in total drag is significant for a commercial aircraft, there are other considerations such as possible increased maintenance cost and application time required to cover the aircraft that have resulted in a very limited number of actual applications of the riblet technology to commercial aircraft. If we are going to see a wide spread application of turbulent drag reduction technologies on commercial aircraft, the turbulent skin friction reductions are going to have to be much larger, perhaps on the order of 20-25%.

In an attempt to obtain much larger drag reductions, the NASA Langley turbulent drag reduction effort is now focused on active turbulent drag reduction concepts. An active system would have three components: sensors, actuators, and controls. In the 1990's there have been numerous CFD studies that showed turbulent boundary layer drag reductions as large as 20-70% for active systems: Choi, Mon, and Kim[35] found up to 25-30 % drag reduction for suction and blowing at the wall; Balogh, Liu, and Krstic,[36] found a 71 % reduction using tangential blowing; Jung, Mangiavacchi and Akhavan[37] found a 40 % reduction for spanwise wall oscillation; and Schoppa and Hussain[38] found a 20 % skin friction reduction using imposed counter-rotating streamwise vortices and a 50 % reduction for colliding spanwise jets.

In CFD studies, control can be exerted at each grid point, which is not possible in a realistic active control configuration. In addition there are physical limitations on the sensors and actuators. As a result there are very few experiments that have actually measured drag reductions with an active control system: Choi, DeBisschop, and Clayton[39] experimentally measured a 45% reduction with spanwise oscillation; and Rathnasingham and Breuer[40] report a 7 % reduction in shear stress using a spanwise array of synthetic jets aligned with the free stream.

Currently NASA Langley is setting up a test bed for an active turbulent boundary layer control system in a low speed tunnel. The test bed will evaluate the performance of an active system using currently available sensors and actuators. The test bed is designed so that various sensors and actuators can be easily substituted. The physical dimensions and layout of the sensors and actuators are sized for interaction with the near wall structure of the turbulent boundary layer. The initial tests will be conducted at 10 m/s. The performance of the active system will be evaluated for various control laws, sensors, and actuators. The goal is to obtain substantial reductions in the turbulent skin friction, determine the flow physics associated with the reductions, and then to scale the skin friction reduction performances to higher velocities and eventually to flight. The early tests will help to determine the characteristics required of the actuator disturbances as well as the required density of sensors and actuators. The first tests are planned for late summer of 2004.

F. Propulsion/Airframe Integration
8. S-Inlet Flow Control

The Blended Wing Body[41] (BWB) vehicle concept has received considerable attention because it shows great promise for improved efficiency. The BWB provides a 19% reduction in operating empty weight and a 32% reduction in fuel burn compared to an advanced long-range transport concept[2]. It achieves these benefits based on the configuration design and vehicle layout and does not resort to advanced materials, structures, or aerodynamics. One of the key features of the original design was the placement of the engines and boundary layer ingesting (BLI) inlets near the aft upper surface of the vehicle. It was conjectured that the inlets in this position would be swallowing the large boundary layer developing over the wing and provide a substantial improvement in drag. The boundary layer on the BWB is expected to be approximately 30% of the inlet height, and that provides a significant challenge in airframe and propulsion integration. All the possible tradeoffs between weight savings and penalties due to reduced engine performance must considered and weighed against any possible drag improvement before the BLI inlet will make it on the configuration. Gorton[42] et al describes a focused effort of developing active flow control technology for BLI S-inlets typical of the BWB. The effort included an assessment of the benefits of BLI from a first principles analysis, the development and validation of computational tools, and control theory for controlling the distortion generated by a BLI inlet. Using a control volume approach a comparison was made between a BLI inlet and a baseline pylon-mounted inlet. The combined effects of BLI and engine cycles were analyzed using the Breguet range equation using a baseline 450-passenger vehicle. The method used in reference 42 assumes that active flow control will decrease the inlet distortion to a commercially acceptable level of 10% using a DC60 criteria. In that manner the analysis only assesses the impact of ingesting the boundary layer. Their analysis showed that for the bypass ratio 10 engines currently in use, the expected improvement in range was approximately 13%. This makes BLI inlets an attractive target for active flow control.

The UEET program also was interested in determining the capability of the current SOA in CFD predictive capability for S-inlets of this type. Berrier[43] and Allan describe an effort to establish a unique high-Reynolds number database for S-inlets. The model was mounted on the wall of the NASA Langley 0.3-m Transonic Cryogenic Tunnel. They evaluated a 2.5% S-duct representative of a BWB for Mach numbers ranging from 0.25 to 0.83, and unit Reynolds numbers from 34×10^6 to 68×10^6 per foot. He determined that increasing the free stream Mach number increased inlet distortion and reduced pressure recovery. Increasing the inlet mass flow had a significant effect on inlet distortion, but only a small effect on pressure recovery. He also found that Reynolds number had a relatively small effect on both inlet distortion and pressure recovery. Using current SOA CFD methods they were able to predict the recovery and distortion trends with increasing Mach number and inlet mass-flow. Berrier and Allan also state that the CFD results were generally more pessimistic than the experimental results (e.g. larger losses).

Figure 13 Front view of inlet mounted in the BART ceiling

Additional research was required to prove that active flow control could reduce the distortion in a BLI inlet and support the assumptions made in the benefits analysis. The UEET propulsion airframe integration project included a small-scale demo of active flow control on a 6% scale model of a 30% BLI diffusing inlet. The test was conducted in the BART tunnel at a freestream Mach number of 0.15 with scaled inlet mass flows for that test condition. The model was designed to fit into the ceiling of the tunnel as shown in Figure 13. The model was instrumented with static pressure ports along the top, bottom, and sides of the duct. It also had a 40-probe total pressure rake (visible in Figure 13) and positioned at the AIP to measure total pressure and distortion in conformance with the SAE standard.

The investigation compared passive flow control techniques using micro vortex generators (MVGs) to active flow control using pulsed jets. MVGs have already been shown to be successful in controlling distortion in S-inlets[44] and highly compact inlets[45] and in this investigation, MVGs provided the baseline against which the pulsed jets would be compared. The details of the MVG and pulsed jet devices and conditions are provided by Gorton et al in reference 42.
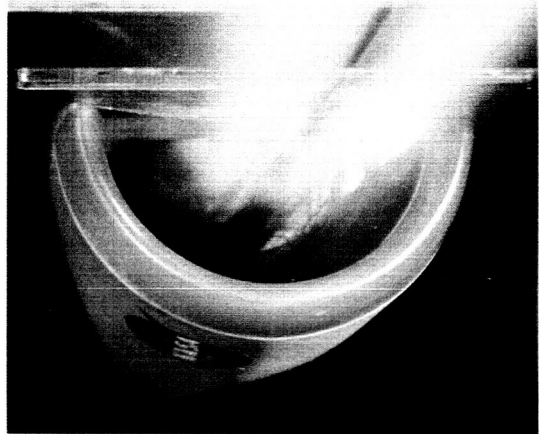
Active flow control provided significant benefits to the performance of the S-inlet. The distortion levels for the baseline uncontrolled case was 29% using the DC60 method. The non-optimized array of MVGs provided a reduction in distortion levels to approximately 11 percent. As described by Gorton in reference 42, there were two constraints placed on the experimental investigation. The first was that the active flow control system could use no more than 1% of the inlet mass flow. The second was that for successful commercial application levels the inlet distortion had to be no greater than 10% when computed using the DC60 method. Figure 14 shows the results of the investigation and provides two important pieces of information. The first was that at the conditions tested, a minimum mass flow of approximately 0.4% was required to reach the 10% distortion level goals. The second was

that a minimum distortion of 4.6% could be achieved with inlet mass flows of 0.55 percent. Gorton et al also demonstrated the use of closed loop control to establish and hold a commanded distortion level. Using CFD methods to establish the sensitivities and to determine possible sensor locations, reference 42, showed that a pressure sensor in the wall could be used in a closed loop system that allows the actual distortion level to track the commanded distortion level very closely.

The research team plans to continue the development of both CFD and experimental databases and methods. Waithe[46] recently implemented a source term model for MVGs and validated the model against a fully gridded MVG as well as experimental data obtained during the UEET program. The source term model has been included in the latest production release of the OVERFLOW code. Work is underway toward the development of a model for the steady and pulsed jets. Current plans are to take the active flow control technology to the higher Mach number cases tested by Berrier in reference 43. CFD methods are being applied to determine the optimum location of the pulsed jet actuators and the required actuator mass flows.
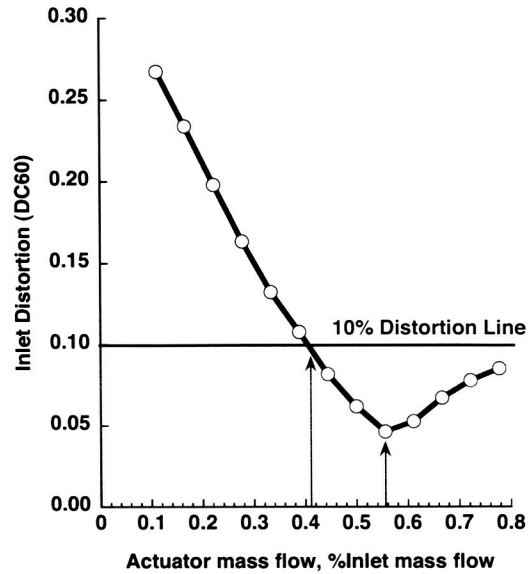

Figure 14 Actuator mass flow sweep (from Ref 42)

G. Maneuvering

9. Stingray

Zero-mass active separation control has been demonstrated to be able to significantly modify the pressure distributions on airfoils that are normally stalled or near stall for lift enhancement and drag reduction. In this project, these ideas for modifying pressure distributions are being exploited on a highly three-dimensional flowfield to explore the effectiveness of active separation control for controlling vehicle moments. The particular platform is the Boeing Stingray, a flying wing UAV, described by Parekh and Glezer[47]. The vehicle, shown in Figure 15, has 50° leading edge sweep and subsonic airfoil sections. Control of the vehicle is achieved by a combination of inner and outer split flaps and leading edge arrays of zero-mass jets. In preparation for closed-loop flight tests, a full-scale wind-tunnel model was built and tested for aerodynamic properties and simulation modeling in the NASA Langley Transonic Dynamics Tunnel and the NASA Langley 14 x 22-ft Low-Speed Tunnel. Georgia Tech Research Institute (GTRI) under contract to NASA conducted sub-scale investigations of this flow-field prior to the full-scale tunnel tests. The full-scale wind tunnel model (built by GTRI) was tested collaboratively between NASA and GTRI. Parekh[48] et al, describe the vehicle configuration, the basic vehicle aerodynamic properties and the integrated response of the vehicle to separation control from the first wind-tunnel test. The time-dependent characteristics and
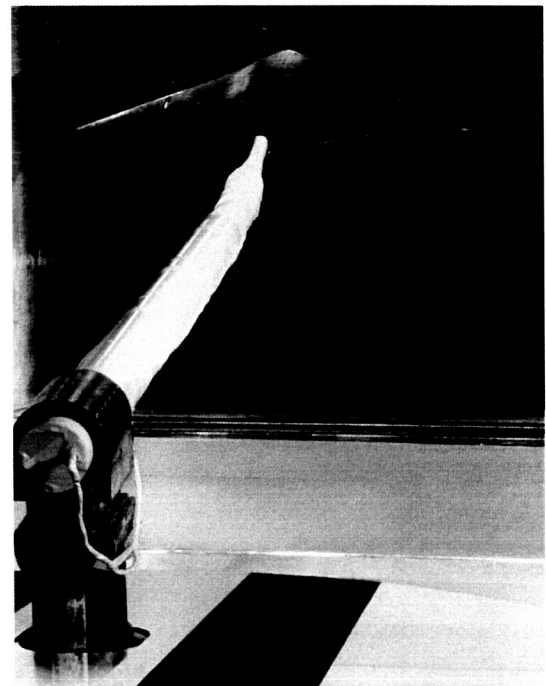

Figure 15 Photo of full-scale Stingray model installed in Langley 14 x 22-ft tunnel

underlying physical mechanisms of the separation control are described in Amitay[49] et al, and Washburn and Amitay[50].

On the Stingray vehicle the application of leading edge separation control yields several intriguing interactions. The region of naturally occurring separation moves from the wingtips inboard as the angle of attack is increased. Mini-tuft flow visualization shows that separation on the outboard wing occurs at angles of attack as low as 12° and progresses to a location inboard of 40% span by 24°. The mini-tufts also did not indicate the presence of a leading edge vortex system with flow control on or off. Since a large portion of the overall lift is generated by the center section of the vehicle, the stall characteristics of the configuration are very mild and lift is not significantly lost even at 24° angle of attack. This effect also limits the effect of the flow control on lift since the outboard region of the wing where the flow is normally separated only accounts for about 25% of the planform area. However, through control of the pressure distributions on the outer portions of the wings significant control authority is possible on pitch, roll, and yaw. The overall integrated effect on the forces and moments is very dependent on the nature of the interaction of this region with the zero-mass jets. The ability to locally affect pressures coupled with the large leading edge sweep works especially well for the control of the pitching moment.

For the purposes of this discussion, the focus will be on the effect of the active separation control on the rolling moment of the vehicle as compared to the level of control generated by the flap system. For the results presented here, the individual jets are operated in unison on each wing to uniformly apply forcing at the leading edge. The jets are pulse modulated at frequency f_m, with only one period of the carrier frequency applied to the jets per pulse. In this mode of operation, the peak velocity from the jets was in the range of 15-18 m/s. Figure 16 shows the effect of flap deflection angle and separation control on the port wing only. Notice that at this angle of attack, the effect of separation control is as large or larger than the effect of the flap deflection. The effects superimpose because the separation control affects the wing performance but does not improve the flap performance increment since control is applied at the wing leading edge. Figure 16 also illustrates perhaps the most significant finding of this project, the degree to which the control level can be varied by changing modulation frequency alone. When the modulation frequency is varied from 22.5 Hz to 90 Hz at constant jet amplitude, the amount of rolling moment varies, even to the point that the sign of the effect is reversed. This effect is repeatable and robust, but the fact that separation control can lower the circulation in a post-stall condition is not necessarily intuitive.

The relative levels of rolling moment control authority from both flaps and separation control over the range of angles tested is approximated in Figure 17. This data shows, that the separation control becomes more effective as the primary interaction location moves inboard where the chord length is greater at the large angles of attack. At the higher angles of attack, where the flaps lose effectiveness, the contribution of AFC to the rolling moment is large. The moment due to AFC can be increased further as shown by operating the jets on one wing at low f_m, and the other wing at high f_m. The final result is a vehicle that has greater roll authority at high angles of attack than at low angles of attack. At angles of attack between 12° and 16° the increment available due to flow control is on the order of the increment that the outer flap contributes to the total moment. At these angles, the effect of AFC is confined to the outer wing where separation naturally occurs.

Figure 16 Contributions of flap deflection and AFC on port wing to rolling moment
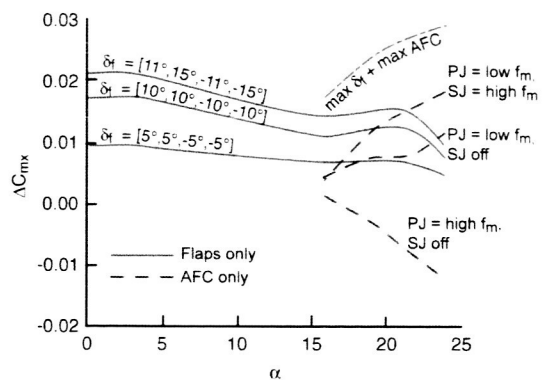
Figure 17 Comparison of AFC to flap authority for rolling moment

The time-averaged surface pressure plot shown in Figure 18 begins to explain what is occurring and causing the sensitivity to f_m in the forces and moments. These data were obtained for surface pressures near 55% of the span
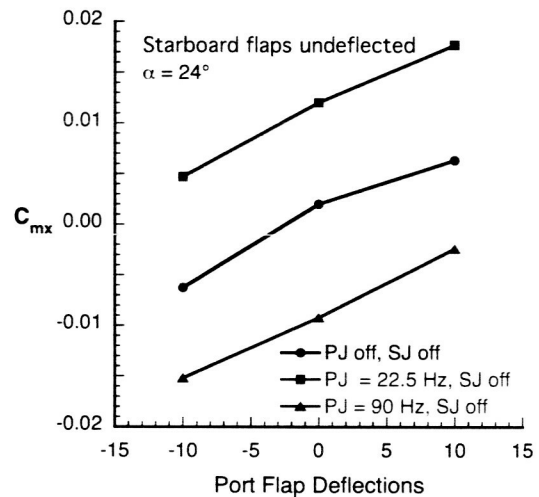
(from x/c from 0 to 0.2, the ports are arranged normal to the leading edge). As the flow is forced at low f_m, like 15 Hz, the time-averaged suction on the upper-surface is increased, but there is no evidence of a suction peak at the leading edge. The effect persists over a large region of the chord as the flow separates and reattaches in a periodic fashion (dynamic lift). This yields an increase in the time-averaged circulation and is a global effect. This could be called control of separated flow. As f_m is increased further to 22.5 Hz and 45 Hz, the development of a suction peak at the leading edge is observed, while the unsteady region of influence is still large in the streamwise direction. The forcing is still coupling to the wake at these f_m. Finally, as f_m is increased to 90 Hz, the development of the suction peak occurs. In this case however, the coupling with the wake does not occur and the effect is very localized and does not persist in the streamwise direction. In this case the flow is very stable and the oscillations very small. This is an example of control of separation (the suction peak develops) but the overall circulation is actually decreased from the baseline. Thus the reversal of the rolling moment with respect to increasing f_m is explained. Further discussion of the time-dependent nature of these phenomena can be found in Washburn and Amitay[50] and Amitay[49] et al, with initial explanation of the transient nature found in Amitay and Glezer[51]. At high angles of attack the lift can be both increased and decreased by about 10% of the baseline. This effect can be used to maintain a fairly constant lift level during a roll setting by operating one wing at low f_m and the other wing at high f_m. Finally, level of control obtained by AFC varies proportionally with respect to the amplitude of the zero-mass jets over a range of input forcing.
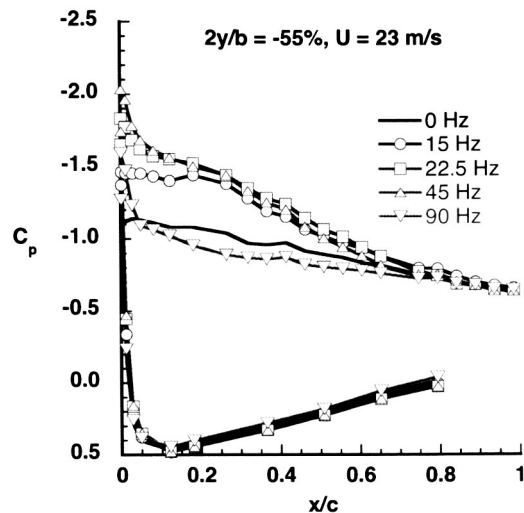

Figure 18 Effect of f_m on time-averaged pressure distribution at $\alpha = 22°$

This effort supports NASA's VSP in two ways. First it provides an opportunity to investigate the feasibility of using distributed, small control devices to maintain vehicle control at low speeds where vehicle control is troublesome. This is especially important for some of the challenges facing the *ESTOL* vehicle class. Secondly, since this investigation is being conducted on a vehicle with large leading edge sweep, it provides useful information regarding the application of active separation control to high lift on S^4T vehicles.

10. Fluidic Thrust Vectoring

Active flow control can provide significant benefits when applied to advanced nozzles. Simpler and lighter nozzles with less moving parts are possible, and thrust vectoring can be used to provide additional control authority as well as an additional component of propulsive lift. Much of Langley's prior work was directed toward nozzle designs for high-performance military vehicles, but vehicles in the S^4T sector can also utilize this technology.

Deere[52] provides a summary of the fluidic thrust vectoring research at Langley with an extensive list of references for many of the techniques. Flow control in nozzles can be used to control throat area, expansion ratio, and thrust-vector angle and Langley's efforts have primarily been focused in the thrust-vectoring arena. Deere divides thrust vectoring into three categories: shock vector control, throat shifting, and counterflow techniques. The potential benefits of fluidic thrust vectoring were provided by Deere, and based on results from the NASA and USAF Fluidic Injection Nozzle Technology (FLINT) program. The program estimated a 28 to 40% weight reduction for throat area control, a 43-80% weight reduction when coupling throat area with exit area control, and a 7 to 12% improvement in engine thrust to weight ratio. She describes the extensive effort over the last 10 years toward obtaining data from the Jet Exit Test Facility (JETF) and the comparisons with computational results. The JETF has been used to obtain static or wind-off data for many of these techniques, and CFD was used to assess the effects of adding a freestream flow component. The reader is referred to reference 52 for a comparison of the various techniques.
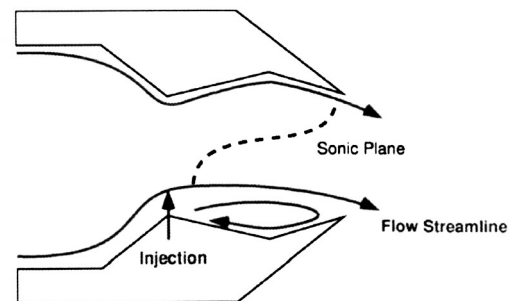

Figure 19 Side view of Recessed Cavity Nozzle (from Ref. 52)

Recent work at Langley has been focused on improving the throat shifting technique using a novel Recessed Cavity Nozzle (RCN). The RCN couples separation control by adding a recessed cavity downstream of the throat. Secondary air is injected upstream of the cavity to induce flow separation. This causes a differential pressure on the upper and lower walls of the nozzle that vectors the primary jet to provide pitch control. A schematic of the configuration is shown in Figure 19. The results to date have been very promising with large thrust vector angles being generated with a minimal impact on thrust efficiency. Thrust vector angles approaching 15° have been obtained with a thrust vectoring efficiency of 2.15° per percent of injection. Computational predictions of the Mach contours and shadowgraph from the JETF experiment are shown in Figure 20 and Figure 21 respectively.

The research has shown that the cavity allowed much lower wall pressures, which resulted in higher thrust deflection angles than could be achieved by other throat shifting methods. Vectoring an isolated nozzle is a beginning, but there are other integration issues involved when putting the nozzle in a configuration. The research effort has included a study of various nozzle aft decks to assess some of those integration issues. A variety of configurations were investigated that included straight and various types of tangent arcs. A 0° straight aft deck was found to be detrimental, but a 20° straight aft deck achieved thrust vectoring efficiencies, h, ranging from 1.7° to 3° per %-injection. Deere et al[53] published the results of an extensive computational study that included design variables such as cavity convergence angle, cavity length, and injection angle. What was found was that shifting the sonic line was not important. Controlling separation in the recessed cavity was the key. The best thrust vector efficiency was obtained with the largest fluidic injection angle in opposition to the flow. A shadowgraph photograph of the RCN without an aft deck installed is shown in Figure 21. Future research in fluidic thrust vectoring at Langley may include investigations of the effect of pulsed injection coupled with new combustion driven actuators.
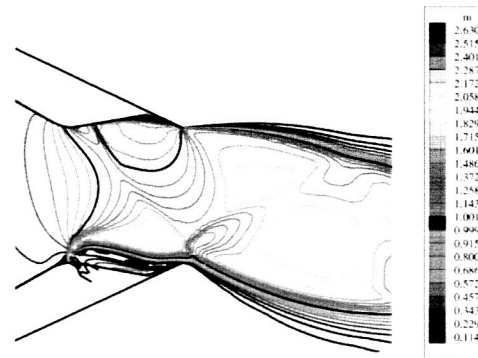

Figure 20 Mach contours for the RCN nozzle with 6% injection

Figure 21 Shadowgraph of the RCN nozzle with 6% injection

H. Physics-Based Modeling

In future visions of aeronautics described in references 1 and 2; the need for improvements in computational predictive capability was deemed essential. Unsteady flows were to play a critical part of that future vision and nowhere is it more evident than in the fields of active flow control. Time accurate CFD methods and turbulence models need to be developed and validated for flows typical of applications of active flow control.

In March of 2004, NASA Langley hosted a Workshop on CFD Validation of Synthetic Jets and Turbulent Separation Control[54] (CFDVAL2004) in Williamsburg, Virginia. One of the over riding goals of the workshop was to assess the current SOA in CFD predictive capability for unsteady flows and separation. The approach was to develop a series of test cases that would, hopefully, provide an unambiguous data set for verifying the codes and their modeling. Three test cases were developed, in collaboration with CFD researchers that were designed to tax the limits of current CFD capability and include a staged increase in geometric and flow physics complexities. The experiments were designed specifically as CFD validation cases, so a great deal of effort was expended to quantify as many of the boundary conditions and experimental uncertainties as possible. This required a change in mindset for the flow control researchers. The goals were NOT to demonstrate the highest performance synthetic jets for flow control technology, but to provide the detailed experimental data necessary for defining the conditions for CFD. The difficulty for the experimental researchers was that the measurement of these unsteady flows also pushed the SOA. Not all of the experimental uncertainties are known with some of the techniques, so in an effort to at least provide a measure of confidence, the flow field parameters were measured with multiple, but complementary techniques. For example, hot-wires, laser velocimetry (LV), and 2D and 3D (Stereo) digital particle image velocimetry (PIV) were used where ever possible and the results compared and presented. Each measurement technique has its advantages

and disadvantages that make direct comparison sometimes difficult in these highly unsteady flows. The sheer volume of data was tremendous and several of the test cases acquired unsteady flow field data sets on the order of a Terabyte in size.

A brief description of the three test cases is provided below, and the reader is encouraged to refer to Yao[55] et al, Schaeffler[56] et al, and Greenblatt[57] et al for detailed descriptions of the experiments and the results. The three test cases included: a synthetic jet in a quiescent flow, a synthetic jet in a crossflow, and separation control of the flow
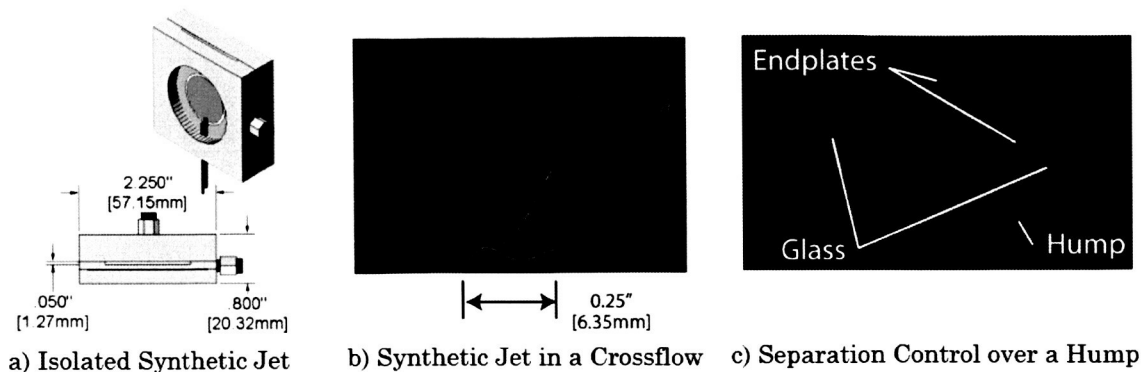

a) Isolated Synthetic Jet   b) Synthetic Jet in a Crossflow   c) Separation Control over a Hump

Figure 22 Test cases for CFDVAL 2004

over a wall-mounted hump. The three test cases are illustrated pictorially in Figure 22. The actuator for case 1 shown in Figure 22a, was a 2 inch diameter, circular, side-mounted piezoelectric diaphragm, that pumped fluid in an out of a rectangular slot 0.50 inch wide and 1.4 inch long. The diaphragm was driven at a frequency of 447 Hz. The pressure, temperature, and diaphragm displacement were simultaneously sampled with all flow field measurements. The synthetic jet issued into quiescent air in a glass-enclosed box 2 ft per side. Phase locked hot-wire, LV, and 2D PIV measurements were obtained of the unsteady jet flow. The instantaneous PIV images showed the flow structure from the slot exit to be very unsteady, raising questions regarding whether the measurements were of turbulence or large-scale motion or "flapping" of the jet. Averaging the PIV images provided a very smooth and detailed image of the vortex structure and velocity profile from the slot as shown in Figure 23. Case 1 also provided an assessment of the errors associated with various "seeding" systems for the LV/PIV systems. Smoke and polystyrene latex

Figure 23 typical flow patterns from slot exit for Case 1

(PSL) particles are typically used for these techniques. The comparison showed that significant differences occurred in the regions 6 mm above the slot. The differences were dependent on the phase angle of the excitation waveform, and therefore on the accelerations or velocity gradients in the flow.
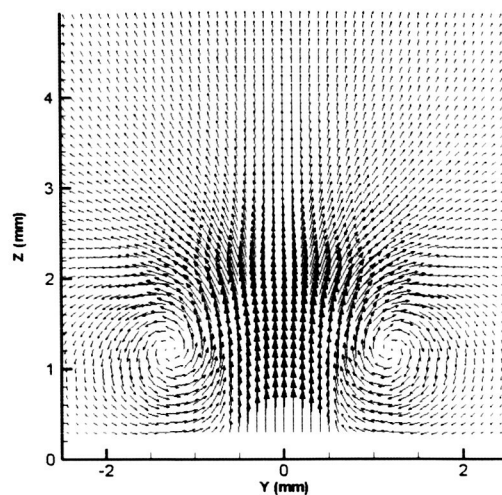
Test case 2 provided the additional complication of the synthetic jet issuing into a turbulent crossflow with zero pressure gradient boundary layer. Figure 22b represents the complex interaction of the synthetic jet interacting with the boundary layer. The actuator used in Case 2 was electro-mechanical and drove a flat piston from the bottom of the cavity. The piston oscillated at a frequency of 150 Hz. The jet emanated from a 0.25-inch diameter orifice into a freestream flow of 34.6 m/s (M=0.1). The maximum velocity out of the orifice was approximately 43 m/s, which provided jet velocity ratios slightly greater than one. The actuator was mounted on the bottom of a splitter plate and the wind tunnel walls adjusted to provide a zero pressure gradient. The incoming boundary layer was approximately 21 mm high. The pressure, temperature, and displacement of the piston were measured as before. Flowfield measurements were obtained with LV and, 2D and 3D PIV systems. Of all three test cases, this one had the additional difficulty in that it was highly three-dimensional. The interactions of the jet and the incoming boundary layer were complex, and there were significant interactions of the freestream flow with the flow in the orifice. This made the assumption of a top hat or Gaussian profile out of the orifice impossible. Figure 24 shows that in the time average what emerges are the typical crossflow vortices found when a steady jet issues into a crossflow.

Test case 3 was geometrically similar to the wall-mounted hump previously investigated by Seifert and Pack[58] at high Reynolds numbers. The hump, shown in Figure 22c, is essentially the upper half of a 20% thick Glauert-Goldschmied airfoil faired onto a 0.5-inch splitter plate. It was tested in the Langley 20 x 28 inch low-speed tunnel at a freestream speed of M = 0.1. The model is 23 inches wide between endplates and has a blowing slot located at the 65% chord location that extends across the entire span of the model. Test case 3 employed 2D/3D PIV and hot-wire anemometers to characterize the flowfield. This test case had three test conditions representing baseline (uncontrolled), steady suction, and zero net mass oscillatory blowing. The steady suction case used a flow meter to provide suction rates of $\dot{m}$ = 0.01518 kg/s through the slot. The increased pressure recovery and reduced separation bubble is shown in Figure 25. The first two conditions were mandatory for the workshop and the third was optional. The oscillatory blowing case used a series of electro-mechanical actuators, operating at a frequency of 138.5 Hz, to drive a rectangular, rigid piston in a deep cavity in the model and provided a maximum velocity at the slot exit of 27 m/s. In addition to the flowfield measurement, case 3 also provided floor and ceiling pressure distributions, dynamic pressures in the separation region and flow visualization of the reattachment region using oil film interferometry.

Rumsey[59] et al provides an overview of the workshop and a summary of the computational results and the reader is referred to his paper for the details. In general there were 75 participants at the workshop from 7 different countries. Most of the participants were from universities, but many private companies and government laboratories were represented as well. He provides details of the organizations, methods, turbulence models, and grids used for each case. Many participants ran several computational cases (e.g. different models) for each experimental test case.

Rumsey et al points out that the time dependent flows featured in the workshop are not only difficult to compute, but also to measure, therefore the workshop ended up as much a workshop on experimental issues as computational issues. The differences on both sides were reported openly in the workshop to provide insight into how to improve future results. He states that because the participants were allowed to run their own grids and boundary conditions, it makes it difficult to sort out specific issues, but comparisons can still be made. Rumsey states: "The bottom line from the CFD results can be summed up in one sentence as follows: no one CFD technique excelled above the others, and there was wide variation (especially for time-dependent results), and only qualitative agreement with experiment. In other words, the SOA CFD methods of today are not fully adequate to consistently and accurately
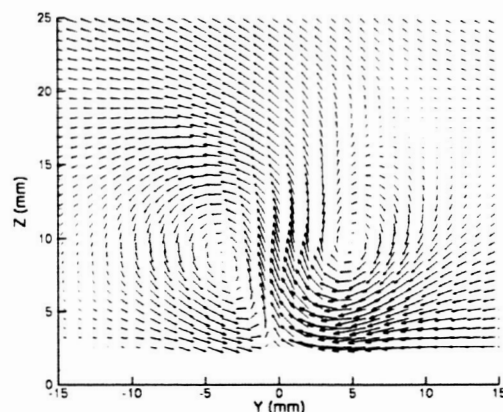

Figure 24 Mean flow pattern 4 jet diameters downstream of the orifice for Case 2
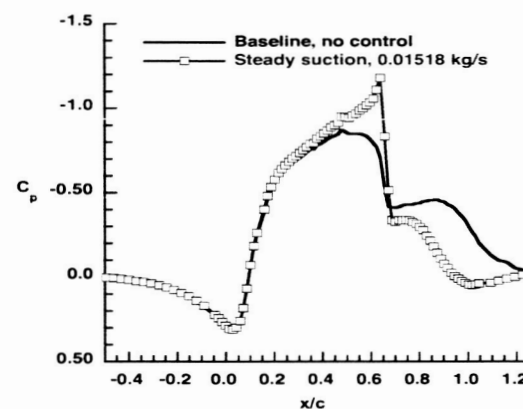

Figure 25 Flow control using steady suction for Case 3

predict these types of flows". He points out that some contributors used higher order methods, but there didn't appear to be any obvious benefit. Some contributors used blended RANS-LES, LES, or DNS that showed some merit, but for the workshop cases they showed no clear benefits over RANS/URANS methods in providing consistently better results for the workshop cases. Rumsey concludes by identifying two areas that are key to improvement. First, for the synthetic jets, it is important to use consistent boundary conditions, and the experimental effort needs to document the extremely time-dependent flowfield variables near the slot exit. Second, for flows with separation like the hump, turbulence models for RANS or hybrid RANS/LES methods need to be improved and calibrated to increase the mixing in the separated region.

IV. Conclusion

A summary of the various active flow control projects at NASA Langley has been presented. The NASA Aeronautics Enterprise has restructured its research efforts, and active flow control research must show clear links with the Vehicle Systems Program goals and objectives. Active flow control is considered an enabling technology for several of the vehicle sectors being investigated. NASA Langley intends to continue pursuing active flow control technology that supports improved high-lift capability, drag reduction, propulsion/airframe integration, and maneuvering performance. There is a critical need for improved predictive capability for the unsteady flow fields typically associated with active flow control technologies, and Langley will continue to develop and validate new computational methods and models in collaborations with industry and universities.

Acknowledgments

References

[1] "The NASA Aeronautics Blueprint – Toward a Bold New Era of Aviation", URL: http://www.aero-space.nasa.gov/aero_blueprint/index.html

[2] Sellers, William L. III, Singer, Bart A., and Leavitt, Laurence D.: "Aerodynamics for Revolutionary Air Vehicles," AIAA Paper 2003-3785, 21st Applied Aerodynamics Conference, Orlando, FL, June 23-26, 2003

[3] Gad-el-Hak, M., "Introduction to Flow Control", in Flow Control: Fundamentals and Practices, Springer-Verlag, 1998, pp. 1-108.

[4] Lord, W. K., MacMartin, D. G., and Tillman, T. G.: "Flow Control Opportunities in Gas Turbine Engines", AIAA 2000-2234, Fluids 2000, Denver, CO, June 19-22, 2000

[5] Washburn, A. E., S. Althoff-Gorton, and S. G. Anders: "Snapshot of Active Flow Control Research at NASA Langley," AIAA Paper 2002-3155, AIAA 1st Flow Control Conference, St. Louis, MO, June 24-26, 2002

[6] 2003 Strategic Plan, National Aeronautics and Space Administration, NASA Headquarters, NP-2003-01-298-HQ, http://www.nasa.gov

[7] Schneider, Wolfgang: "The Importance of Aerodynamics in the Development of Commercially Successful Transport Aircraft", CEAS/DragNet European Drag Prediction Conference 2000, Potsdam, Germany, 19-21 June 2000.

[8] Wimpress, John K. and Newberry, Conrad F.: "The YC-14 STOL Prototype: Its Design, Development, and Flight Test", American Institute of Aeronautics and Astronautics

[9] Wlezien, R.W. and Veitch, L.: "Quiet Supersonic Platform Program Advanced algorithms for design and optimization of Quiet Supersonic Platforms," AIAA Paper 2002-0143, 40th Aerospace Sciences Meeting, Reno, NV, January 14-17, 2002.

[10] Anders, Scott G, and Fischer, Michael C.: "F-16XL-2 Supersonic Laminar Flow Control Flight Experiment," NASA TP-1999-209683, December 1999.

[11] Marshall, Laurie, A.: "Boundary-Layer Transition Results from the F-16XL-2 Supersonic Laminar Flow Control Experiment," NASA TM-1999-209013, December 1999.

[12] Wimpress, J. K.: "Aerodynamic Technology Applied to Takeoff and Landing", International Congress of Subsonic Aircraft, *Annals of the New York Academy of Sciences*, Vol. 154, Art 2, November, 1968, pp 962-981.

[13] McLean, J. D., Crouch, J. D., Stoner, R. C., Sakurai, S., Seidel, G. E., Feifel, W. M., and Rush, H. M., "Study of the Application of Separation Control by Unsteady Excitation to Civil Transport Aircraft," NASA CR-209338, 1999.

[14] Pack, L. G., Schaeffler, N. W., Yao, C., and Seifert, A.: "Active Control of Separation from the Slat Shoulder of a Supercritical Airfoil," AIAA 2002-3156, AIAA 1st Flow Control Conference, St. Louis, MO, June 24-26, 2002

[15] Melton-Pack, LaTunia, Yao, Chung-Sheng, and Seifert, Avi: "Active Control of Separation from the Flap of a Supercritical Airfoil," AIAA 2003-4005, 33rd AIAA Fluid Dynamics Conference and Exhibit, 23-26 June 2003, Orlando, Florida

[16] Washburn, Anthony, E.: "NASA Micro-Aero-Adaptive-Control," SPIE Paper 4332-39, SPIE 8th Annual International Symposium on Smart Structures and Materials, 4-8 March 2001

[17] Lin, J. C. and Dominik, C. J.: "Parametric Investigation of a High-Lift Airfoil at High Reynolds Numbers," *Journal of Aircraft*, Vol. 33, No. 4, 1997, pp. 485-491

[18] Sellers, W. L. and Kjelgaard, S. O., "The Basic Aerodynamic Research Tunnel – A Facility Dedicated to Code Validation, AIAA-88-1997, 15th Aerodynamic Testing Conference, San Diego, CA, May 18-20, 1988

[19] Melton-Pack, LaTunia, Yao, Chung-Sheng, and Seifert, Avi: "Application of Excitation from Multiple Locations on a Simplified-High Lift System," AIAA 2004-2324, 2nd AIAA Flow Control Conference, Portland, OR, 28 June – 1 July, 2004

[20] Englar, R. J., "Circulation Control Pneumatic Aerodynamics: Blown Force and Moment Augmentation and Modifications; Past, Present and Future," AIAA 2000-2541, AIAA Fluids 2000 Conference, June 2000.

[21] Jones, G. S., Washburn, A. E., Jenkins, L. N., and Viken, S. A., "An Active Flow Circulation Controlled Flap Concept for General Aviation Aircraft Applications," AIAA Paper 2002-3157, 1st Flow Control Conference, June 2002.

[22] Sellers, W.L., Jones, G.S., and Moore, M.D.: "Flow Control Research at NASA Langley in Support of High-Lift Augmentation," AIAA-2002-6006, Biennial International Powered Lift Conference, Williamsburg, VA, November 2002,.

[23] Jones, Gregory S. and Englar, Robert J.: "Advances in Pneumatic-Controlled High-Lift Systems," AIAA 2003-3411, 21st Applied Aerodynamics Conference, Orlando, FL, 23-26 June 2003

[24] Jones, G. S., Joslin, R. D., Proceedings of Circulation Control Workshop, March 2004, Hampton, VA, to be published as a NASA CP

[25] Nielson, J. N., Proceedings of the Circulation-Control Workshop 1986, NASA CP 2432, NASA Ames, CA, February 1986.

[26] Abramson, J., Two-Dimensioinal Subsonic Wind Tunnel Evaluation of Two Related Cambered 15-percent-Thick Circulation Control Airfoils, DTNSRDC ASED-373, September 1977

[27] Novak, C. J., Cornelius, K. C., Roads, R. K., Experimental Investigations of the Circular Wall Jet on a Circulation Control Airfoil, AIAA-87-0155, January 1987

[28] Novak, C. J., Cornelius, K. C., An LDV Investigation of a Circulation Control Airfoil Flowfield, AIAA-86-0503, January 1986

[29] *"Drag Reduction by Shock and Boundary Layer Control: Results of the Project EUROSHOCK II Supported by the European Union 1996-1999"*, edited by Egon Stanewsky, Jean Delery, John Fulker, and Paolo de Matteis, Springer-Verlag, Berlin, 2002

[30] Stanewsky, W.: "Adaptive Wing and Flow Control Technology," *Progress in Aerospace Sciences*, Vol. 37, 2001, pp. 583-667.

[31] Drela, M., "Design and Optimization Method for Multi-Element Airfoils," AIAA Paper 93-0969, Feb. 1993

[32] Campbell, R.L., "Efficient Viscous Design of Realistic Aircraft Configurations," AIAA Paper 98-2539, June 1998

[33] Anderson, W.K. and Bonhaus, D.L., "An Implicit Upwind Algorithm for Computing Turbulent Flows on Unstructured Grids," *Computers in Fluids*, Vol. 23, No. 1., 1994, pp. 1-21.

[34] Milholen, William E. II, and Owens, Lewis R.: "On the Application of Contour Bumps for Transonic Drag Reduction," proposed AIAA Paper, 43rd Aerospace Sciences Meeting and Exhibit, Reno, NV, January 10-13, 2005 (unpublished)

[35] H. Choi, P. Moin, and J. Kim, "Active turbulence control for drag reduction in wall bounded flows," *J. Fluid Mech.* 262, 75 , 1994.

[36] Balogh, A.; Wei-Jiu Liu; Krstic, M. "Stability Enhancement By Boundary Control In 2D Channel Flow. I. Regularity Of Solutions." In Decision and Control, 1999. Proceedings of the 38th IEEE Conference on Volume: 3 , 1999 , Page(s): 2869 –2874.

[37] Jung, W.J., Mangiavacchi ,N., and Akhavan, R.: "Suppression of Turbulence in Wall-Bounded Flows by High-Frequency Spanwise Oscillations," Phys. Fluids A, vol. 4, no. 8, pp. 1605-1607, 1992.

[38] Schoppa, W., and Hussain, F.: "A Large Scale Control Strategy for Drag Reduction in Turbulent Boundary Layers." *Physics of Fluids*, Volume 10, Number 5, May 1998, pp. 1049-1051.

[39] Choi, K.-S., DeBisschop, J.-R. and Clayton, B.R.: "Turbulent Boundary Layer Control by Means of Spanwise Wall Oscillation," *AIAA Journal*, Vol. 36, No. 7, July 1998, pp. 1157-1163.

[40] Rathnasingham, R. and Breuer, K.S.: "Active control of turbulent boundary layers," *J. Fluid Mechanics*, Vol. 495, 2003, pp.209-233.

[41] Liebeck, R.: "Design of the Blended-Wing-Body Subsonic Transport", AIAA-2002-0002, 40th AIAA Aerospace Sciences Meeting, Reno, NV, January 14-17, 2002

[42] Gorton, Susan, Owens, Lewis R., Jenkins, Luther N., Allan, Brian G., and Schuster, Ernest P.: "Active Control on a Boundary-Layer-Ingesting Inlet", AIAA 2004-1203, , 42nd AIAA Aerospace Sciences Meeting and Exhibit, Reno, Nevada, January 5 – 8, 2004,

[43] Berrier, Bobby, L., and Allan, Brian, G.: "Experimental and Computational Evaluation of Flush Mounted, S-Duct Inlets," AIAA 2004-764, 42nd AIAA Aerospace Sciences Meeting and Exhibit, Reno, Nevada, January 5 - 8, 2004

[44] Anabtawi, A. J., Blackwelder, R. F., Lissaman, P. B., and Liebeck, R. H.: "An Experimental Investigation of Boundary Layer Ingestion in a Diffusing S-Duct With and Without Passive Flow Control," AIAA 1999-0739, 37th Aerospace Sciences Meeting and Exhibit, Reno, NV, Jan. 11-14, 1999

[45] Anderson, B.H., Miller, D. N., Yagle, P. J., and Truax, P. P.: "A Study of MEMS Flow Control for the Management of Engine Face Distortion in Compact Inlet Systems," Proceedings of the 3rd ASME/JSME Joint Fluids Engineering Conference, July, 1999.

[46] Waithe, K.: "Source Term Model for Vortex Generator Vanes in a Navier-Stokes Computer Code," AIAA 2004-1236, 42nd Aerospace Sciences Meeting and Exhibit, Reno, NV, January 5-8, 2004.

[47] Parekh, D. E. and Glezer, A., "AVIA: Adaptive Virtual Aerosurface", AIAA 2000-2474, Fluids 2000, June 2000

[48] Parekh, David E., Williams, Stephen P., Amitay, Michael, Glezer, Ari, Washburn, Anthony E., Gregory, Irene M., and Scott, Robert C: "Active Flow Control on the Stingray UAV: Aerodynamic Forces and Moments", AIAA 2003-4002, 33rd AIAA Fluid Dynamics Conference and Exhibit, 23-26 June 2003, Orlando, Florida

[49] Amitay, Michael, Washburn, Anthony E., Anders, Scott G, and Parekh, David E.: "Active Flow Control on the Stingray UAV: Transient Behavior," AIAA 2003-4001, June 2003, Accepted to *AIAA Journal*, April 2004

[50] Washburn, Anthony E. and Amitay, Michael: "Active Flow Control on the Stingray UAV: Physical Mechanisms," AIAA 2004-745, 42nd AIAA Aerospace Sciences Meeting and Exhibit, 5 - 8 January 2004, Reno, Nevada

[51] Amitay, M and Glezer, A; "Controlled Transients of Flow Reattachment over Stalled Airfoils"; *International Journal of Heat Transfer and Fluid Flow*, Volume 23, Issue 5, pp. 690-699, October 2002

[52] Deere, Karen A.: "Summary of Fluidic Thrust Vectoring Research Conducted at NASA Langley Research Center", AIAA 2003-3800, 21st Applied Aerodynamics Conference, Orlando, FL, June 23-26, 2003

[53] Deere, Karen A., Bobby L. Berrier, Jeffrey D Flamm, and Stuart K. Johnson: "Computational Study of Fluidic Thrust Vectoring using Separation Control in a Nozzle", AIAA 2003-3803, 21st Applied Aerodynamics Conference, Orlando, FL, June 23-26, 2003

[54] Langley Research Center Workshop on "CFD Validation of Synthetic Jets and Turbulent Separation Control," URL: http://cfdval2004.larc.nasa.gov

[55] Yao, Chung-sheng , Chen, Fang-Jenq , Neuhart, Dan, and Harris, Jerome: "Synthetic Jet Flow Field Database for CFD Validation," AIAA 2004-2218, 2nd AIAA Flow Control Conference, 28 June - 1 July, 2004

[56] Schaeffler, N. W. and Jenkins, L. N., "The Isolated Synthetic Jet in Crossflow: A Benchmark for Flow Control Simulation," AIAA 2004 - 2219, 2nd AIAA Flow Control Conference, 28 June - 1 July, 2004

[57] Greenblatt, D., Paschal, K. B., Schaeffler, N. W., Washburn, A. E., Harris, J. and Yao, C. S.: " A Separation Control CFD Validation Test Case. Part 1: Baseline & Steady Suction," AIAA 2004-2220, 2nd AIAA Flow Control Conference, 28 June - 1 July, 2004

[58] Seifert, A. and Pack, L. G.: "Active Flow Separation Control on a Wall-Mounted Hump at High Reynolds Numbers," *AIAA Journal*, Vol. 40, No. 7, July, 2002

[59] Rumsey, C. L., Gatski, T. B., Sellers, William L. III, Vatsa, V. N., and Viken, S. A.: "Summary of the 2004 CFD Validation Workshop on Synthetic Jets and Turbulent Separation Control," AIAA 2004-2217, 2nd AIAA Flow Control Conference, 28 June - 1 July, 2004